Surface Active Element Effects on the Shape of GTA, Laser, and Electron Beam Welds

The results of experimentation confirm the surface tension driven fluid flow model for the effect of minor elements on GTA weld pool shape

BY C. R. HEIPLE, J. R. ROPER, R. T. STAGNER AND R. J. ADEN

ABSTRACT. Laser and electron beam welds were passed across selenium-doped zones in 21-6-9 stainless steel. The depth/width (d/w) ratio of a defocused laser weld with a weld pool shape similar to a GTA weld increased by over 200% in a zone where 77 ppm selenium had been added. Smaller increases were observed in selenium-doped zones for a moderately defocused electron beam weld with a higher d/w ratio in undoped base metal.

When laser or electron beam weld penetration was by a keyhole mechanism, no change in d/w ratio occurred in selenium doped zones. The results confirm the surface tension driven fluid flow model for the effect of minor elements on GTA weld pool shape. Other experimental evidence bearing on the effect of minor elements on GTA weld penetration is summarized.

Introduction

Many studies have reported variations in the shape of GTA weld fusion zones in stainless steels and other materials with changes in the concentration of one or more impurities in the base metal (Ref. 1–12). A mechanism for the effect of small concentrations of certain impurities on GTA weld pool shape has recently been presented (Ref. 11). It was proposed that fluid flow in the GTA weld pool is generally the major factor determining fusion zone shape and that the dominant force driving fluid flow under many welding conditions is a surface tension gradient. Surface tension gradients exist on a weld pool surface, because the surface tension is temperature dependent and there are substantial temperature gradients on a weld pool surface.

Small concentrations of surface active elements (that is, elements which segregate preferentially to the surface of the liquid metal) affect weld pool shape by altering surface tension gradients on the weld pool surface and thereby changing the magnitude and/or direction of fluid flow in the weld pool. In addition, impurities which are not surface active may affect weld pool shape. This can occur if they react with surface active impurities (also present in the weld pool) to form compounds which are not surface active, and thus prevent the surface active impurities from influencing surface tension gradients.

In the absence of significant concentrations of surface active elements, the surface tension of molten metals and alloys decreases with increasing temperature (Ref. 13). For GTA welds in such materials, the surface tension will be greatest at the toe (edge) of the weld pool and lowest in the hottest part of the weld pool near the center under the arc. The surface tension gradient, therefore, produces fluid flow outward from the center of the weld pool surface as indicated schematically in Fig. 1A. This fluid flow pattern efficiently transfers heat from the hottest part of the weld pool (under the arc) to the toe of the weld and thereby produces a relatively wide and shallow weld.

The addition of surface active elements to molten metals can drastically change the temperature dependence of the surface tension so that, for a range of temperature above the melting point, the surface tension increases with increasing temperature. In this case, the surface tension is highest near the center (hotter) region of the weld pool. Fluid flow will be

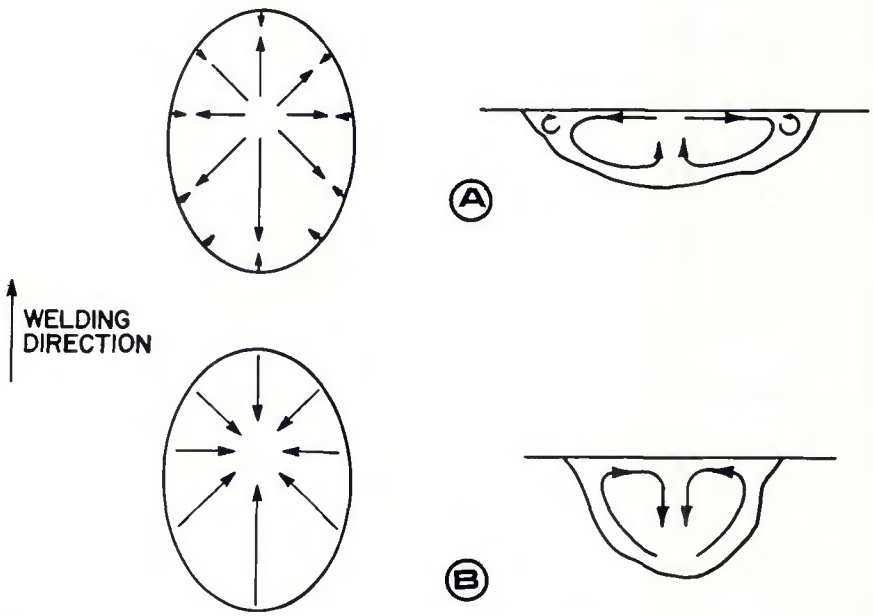

Fig. 1—Proposed fluid flow on and below the weld pool surface: A—negative surface tension temperature coefficient; B—positive surface tension temperature coefficient

C. R. HEIPLE, J. R. ROPER, R. T. STAGNER, and R. J. ADEN are with Rockwell International, Energy Systems Group, Rocky Flats Plant, Golden, Colorado.

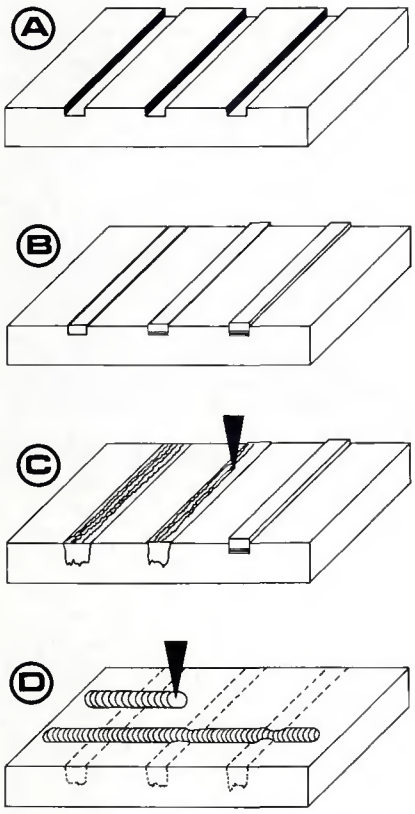

Fig. 2—Procedure for doping 21-6-9 base metal; flattening and milling the plate smooth are not shown. A—machine slots in surface; B—insert foil(s) and cover plates in slots; C—electron beam melt cover plates, foil(s), and some base metal; D—run GTA weld beads across electron beam melted zones

inward along the surface of the weld pool toward the center and then down, as indicated schematically in Fig. 1B. This fluid flow pattern efficiently transfers heat to the weld root and produces a relatively deep and narrow weld.

It is explicitly recognized that the flow patterns shown in Fig. 1 are idealizations. They were inferred from high speed motion pictures of the motion of aluminum oxide particles on GTA weld pool surfaces (Ref. 11). The precise fluid flow pattern is more complicated. The complexity arises, in part, because other forces contribute to fluid flow in the weld pool (primarily the Lorentz and buoyancy forces). Also, the positive temperature coefficient of surface tension only exists over a limited temperature range—which may be exceeded near the center of the weld pool.

The model summarized above for the mechanism by which impurities can affect the shape of GTA welds was derived in part from observations of the effects of sulfur (Ref. 11, 12) and aluminum (Ref. 12) on fusion zone shape in stainless steels. The effects of Se, Te, O_2, and Ce on GTA weld pool shape in stainless steels were predicted using the model and experimental confirmation of these predictions has been reported (Ref. 10, 12).

The model is not restricted to a gas tungsten arc as the heat source. Impurities should produce similar changes in weld pool shape with other heat sources, provided that the energy density and distribution deposited on the weld pool surface is comparable to that from a gas tungsten arc. Changes observed in weld pool shape when laser and electron beam welds crossed zones in 21-6-9 doped with Se are reported here.

Table 1—Analysis of Type 303Se Stainless Steel Foil Used to Dope 21-6-9, Wt-%

Cr	17.48
Ni	9.6
Si	0.67
C	0.04
P	0.17
Mn	1.26
Mo	0.24
Cu	0.20
S	0.022
Se	0.25
Fe	Balance

Table 2—Analysis of 21-6-9 Plate, Wt-%

Cr	20.1
Ni	6.8
Mn	8.7
N_2	0.27
C	0.025
Al	0.0058
O_2	0.0058
S	0.0024
Fe	Balance

Experimental

Strips in a plate of 21-6-9 (25 mm or 1 in. thick) were doped with low concentrations of Se to test the effect of adding a surface active element on the shape and penetration of laser and electron beam welds. Selenium was chosen as the dopant, because it had produced large changes in the shape of GTA welds (Ref. 10) and was easily added to 21-6-9. The doping technique has been described in detail previously (Ref. 2), and has been used to dope stainless steels with Al, S, Se, Te, Ce, and O (Ref. 2, 12) for GTA welding experiments.

The procedure is shown schematically in Fig. 2. Slots 3.2 mm (⅛ in.) deep and 9.5 mm (⅜ in.) wide were machined in plates of 21-6-9 stainless steel. Foils of Type 303Se stainless steel, which contained 0.25 wt-% Se, were placed in the bottoms of the slots. The composition of these foils is given in Table 1. One slot was always left undoped. Cover plates cut from the same plate of 21-6-9 from which the sample was machined were put in all the slots. Multiple passes were then made with an electron beam traveling parallel to the slots, thereby fusing the cover plate, the foils, and part of the base metal. The approximate depth of penetration of the electron beam was 9 mm (0.35 in.).

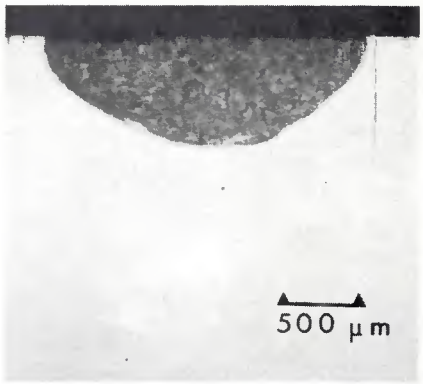

Fig. 3—Cross section of defocused, decoupled laser weld in undoped base metal with focus above 21-6-9 plate surface

The number and thickness of the foils were selected so as to add the desired nominal dopant concentrations, in this case 50, 100, and 150 ppm. Significant vaporization of the dopant occurred during electron beam melting, and the actual concentration of dopant in the beam melted zones was less than nominal. Chemical analyses of the beam melted zones were performed to determine actual dopant concentration.

Selenium was known to produce deep and narrow GTA welds. For this reason, 21-6-9 base metal with a known low GTA d/w ratio was used for the electron beam and laser weld tests. The composition of the 21-6-9 plate used is given in Table 2.

Results

Five different bead-on-plate welds were made across the Se-doped 21-6-9 plate. These were:

1. A defocused, decoupled* laser weld with the focus above the plate surface.
2. A defocused, coupled* laser weld with the focus above the plate surface.
3. A defocused, decoupled laser weld

**There is a gradual increase in the fraction of incident energy absorbed as laser power density incident on a metal surface increases. Absorbance increases sharply for a small increase in power density at a critical power density. At critical power density, the surface temperature of metal is reported to be well above the metal's melting point (Ref. 14). Welds made below the critical power density (low absorbance) are said to be decoupled; welds made above the critical power density (high absorbance) are described as being coupled. Virtually all laser welding applications involve the coupled mode.*

Table 3—Changes in Laser and Electron Beam d/w Ratios in 21-6-9 Doped with Selenium

Weld type	Zone	Se content, ppm	d/w	Increase from undoped zone, %
Defocused, decoupled laser—focus above plate	Base metal	<10	0.32	—
	Base metal, plus 1 foil 303Se	30	0.71	122
	Base metal, plus 2 foils 303Se	77	0.98	206
	Base metal, plus 3 foils 303Se	68	0.82	156
Defocused electron beam	Base metal	<10	0.89	—
	Base metal, beam melted	<10	0.88	—
	Base metal, plus 1 foil 303Se	30	0.98	11
	Base metal, plus 2 foils 303Se	77	1.08	23
Defocused, decoupled laser—focus below plate surface	Base metal	<10	0.67	
	Base metal, beam melted	<10	0.65	
	Base metal, plus 1 foil 303Se	30	0.65	
	Base metal, plus 2 foils 303Se	77	0.65	
	Base metal, plus 3 foils 303Se	68	0.69	

with the focus below the plate surface.

4. A defocused electron beam weld.

5. A normal, sharply focused, deep penetration (11 mm, i.e., 0.43 in.) electron beam weld.

Of the five welds attempted, the one most closely resembling a GTA weld was the defocused, decoupled laser weld with the focus above the plate surface. A cross section of this weld in undoped base metal is shown in Fig. 3. The weld is considerably smaller than the GTA welds reported previously (Ref. 10-12).

A large change in weld shape occurred in the doped zones. The cross section in the zone where two foils of Type 303Se stainless steel had been added is shown in Fig. 4. The d/w ratios are given in Table 3. The change in shape of the defocused laser weld when it crossed a Se-doped zone was similar to that observed previously for GTA welds when they crossed zones doped with surface active elements (Ref. 10, 12). (The shapes of GTA welds in undoped and sulfur- or tellurium-doped zones in 21-6-9 are shown in Figs. 5–8 for comparison.) The selenium-doped zones for the laser and electron beam weld tests were analyzed for selenium, and the results are also included in Table 3. The maximum selenium concentration achieved for this experiment was 77 ppm.

The d/w ratio of the defocused electron beam weld in undoped regions was considerably higher than typical GTA welds in plate of the same composition. There was a modest increase in d/w ratio when the defocused electron beam crossed selenium-doped zones. Changes in the d/w ratio resulted almost entirely from changes in the width of the weld.

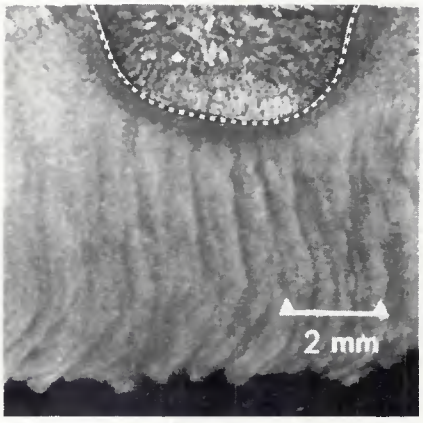

Fig. 6—GTA weld cross section in a sulfur-doped electron beam melted zone in 21-6-9 containing 80 ppm S; fusion zone boundary outlined for clarity

Cross sections of this weld in undoped and doped electron beam melted zones are shown in Figs. 9 and 10, and the d/w ratios are given in Table 3. (No value for the zone with three foils added is given because gross surface cavities prevented a reasonable measurement of weld cross section. Neither surface cavities nor included porosity were observed for electron beam welds crossing the other doped zones.)

The penetration mechanism in a sharply focused electron beam weld is completely different than in a GTA weld. No change in the depth of penetration or bead width was seen in the focused electron beam when it crossed a selenium doped zone. A longitudinal section of the electron beam weld where it crossed a selenium-doped zone is given in Fig. 11.

Similar results were observed for the coupled, defocused laser weld and the uncoupled, defocused laser weld with the focus below the plate surface. A keyhole apparently formed for the coupled, defocused laser weld, and neither the maximum depth of the weld nor its

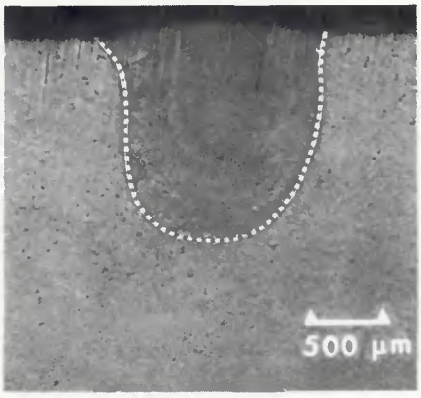

Fig. 4—Cross section of defocused, decoupled laser weld with focus above plate surface in a selenium-doped electron beam melted zone in 21-6-9; fusion zone boundary outlined for clarity

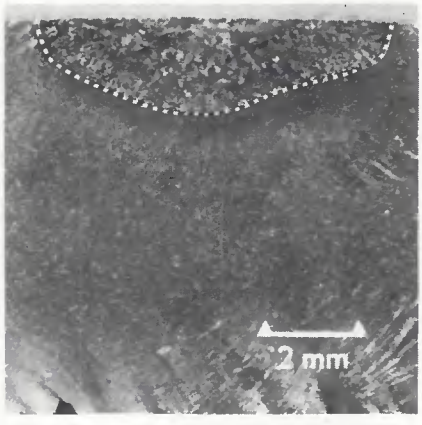

Fig. 5—GTA weld cross section in an undoped electron beam melted zone in 21-6-9 containing 30 ppm S; fusion zone boundary outlined for clarity

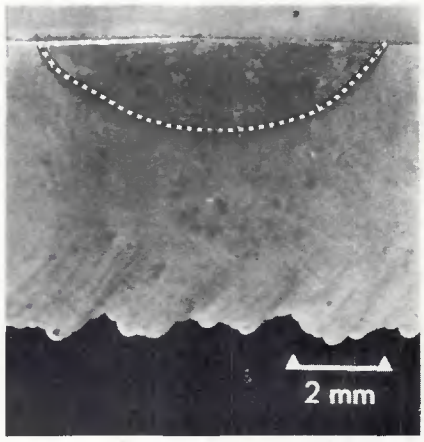

Fig. 7—GTA weld cross section in an undoped electron beam melted zone in 21-6-9; fusion zone boundary outlined for clarity

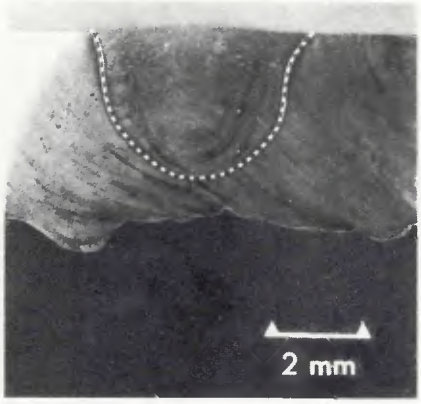

Fig. 8—GTA weld cross section in a tellurium-doped electron beam melted zone in 21-6-9 containing 62 ppm Te; fusion zone boundary outlined for clarity

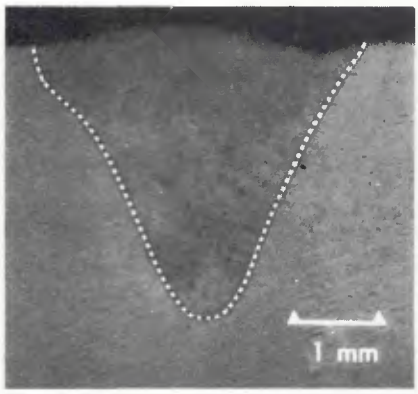

Fig. 9—Cross section of a defocused electron beam weld in an undoped, beam melted zone in 21-6-9; fusion zone boundary outlined for clarity

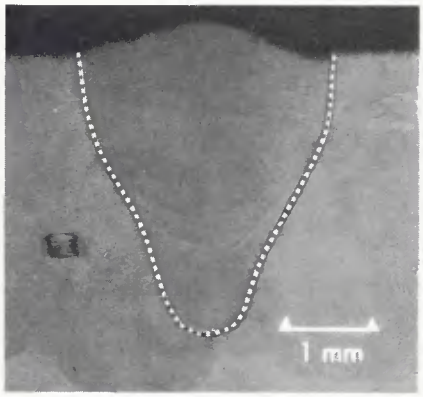

Fig. 10—Cross section of a defocused electron beam weld in a selenium-doped, beam melted zone in 21-6-9; fusion zone boundary outlined for clarity

width changed in the doped zones. The peculiar cross section of this weld is shown in Fig. 12. It is unclear that the d/w ratio for a weld of this shape has any significance, and it is not listed in Table 3.

Finally, no change in the d/w ratio of the uncoupled laser weld with the focus below the plate surface occurred when the weld crossed selenium-doped zones. A representative cross section of this weld in the undoped, beam melted zone is given in Fig. 13 and the d/w ratios achieved are listed in Table 3.

Discussion

The surface tension driven fluid flow model predicts that minor elements will similarly affect the shape of GTA weld pools and weld pools created by some heat sources other than a gas tungsten arc, provided that the input energy density is low enough that a keyhole is not formed. A dramatic increase in weld d/w ratio was observed when a defocused, decoupled laser weld with the focus above the plate was passed across selenium doped zones in 21-6-9. The changes observed in d/w ratios were comparable to those observed previously for GTA welds. A considerably smaller change in d/w ratio occurred when a defocused electron beam crossed selenium-doped zones. The d/w ratio for this weld was fairly high in undoped base metal; consequently, d/w increases in selenium doped zones were correspondingly smaller.

When laser and electron beam penetration was by a keyhole mechanism, selenium doping at the low concentrations (<80 ppm) tested had little effect on weld shape. It is generally believed that surface tension forces are important in determining the depth and stability of the keyhole. The important parameter may be the magnitude of the surface tension, rather than surface tension gradients arising from the temperature dependence of the surface tension. Small concentrations of surface active elements alter the magnitude of the surface tension as well as the temperature dependence. However, the change in the magnitude of the surface tension may be too small to affect the keyhole.

Any proposal which seeks to explain the effects of trace impurities on the shape or penetration of GTA welds must account for, or be consistent with, quite a number of experimental observations (mostly on stainless steels). These observations are summarized below and discussed in terms of the dominant mechanism determining weld pool shape being fluid flow driven by surface tension gradients. Other mechanisms are consistent with one or more of these observations. However, it appears at present that only the surface tension driven fluid flow mechanism is consistent with the entire set of observations.

Sulfur, oxygen, selenium, and tellurium are surface active and are either known (S and O) or expected (Se and Te) to produce a positive temperature coefficient of surface tension in iron at very low concentrations. The model, therefore, predicts, solely on the basis of the available surface tension data, that all these elements will increase GTA weld penetration in steels; all of them have been shown to substantially increase penetration in 21-6-9 (Ref. 12). Sulfur has also been shown to increase penetration in Type 304 stainless steel (Ref. 15). Furthermore, the concentrations required to substantially affect weld shape are so small that significant alteration of bulk properties (such as viscosity or thermal conductivity) of the weld pool or base metal is highly unlikely. For example, only

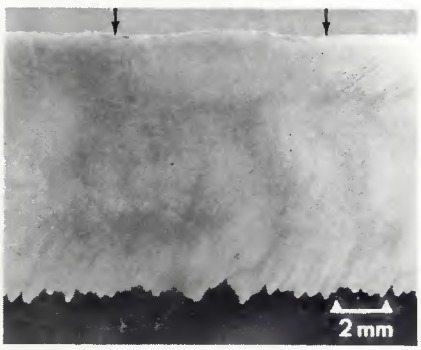

Fig. 11—Longitudinal section of a sharply focused electron beam weld crossing a selenium-doped, beam melted zone in 21-6-9. The Se-doped zone lies approximately between the arrows

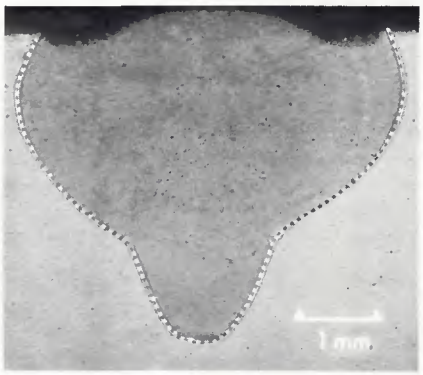

Fig. 12—Cross section of a defocused, coupled laser weld in 21-6-9; fusion zone boundary outlined for clarity

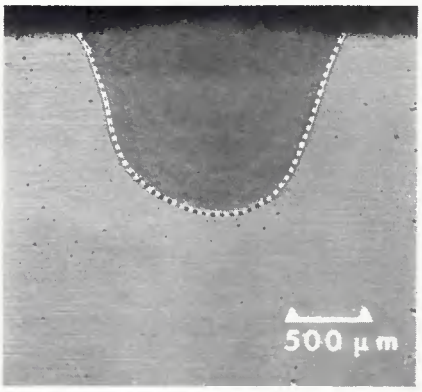

Fig. 13—Cross section of a defocused, decoupled laser weld with the focus below the plate surface in 21-6-9; fusion zone boundary outlined for clarity

the addition of 40 ppm Se was required to increase the d/w ratio of GTA welds in 21-6-9 by 80% (Ref. 10).

Since S, O, Se, and Te are known to segregate to the surface of liquid iron, surface properties can be altered substantially by low average bulk concentrations of these elements. Because quite low concentrations of surface active elements are adequate to produce a positive surface tension temperature coefficient and good penetration, poor penetration is normally expected only in steels particularly low in sulfur, as observed.

It should be noted that one aspect of the effect of oxygen on weld pool shape is puzzling. As predicted, small concentrations of oxygen dissolved in 21-6-9 stainless steel base metal increase the d/w ratio of GTA welds (Ref. 12). Furthermore, Fihey and Simoneau (Ref. 16) observed a substantial increase in GTA weld penetration in a low sulfur, low oxygen Type 304L stainless steel when 0.1% oxygen was mixed into the argon shielding gas. However, when they added 1.0% oxygen to the shielding gas, the weld pool returned to a wide, shallow cross section, essentially identical to that observed for a pure argon shielding gas (Ref. 16). The return to poor penetration at high oxygen concentrations in the shielding gas was attributed to changes in the anode spot size. Another possibility is that a high oxygen level in the shielding gas results in the formation of a (liquid) oxide layer on the weld pool surface which alters the surface tension gradients.

Cerium and aluminum are not surface active in iron, but aluminum is known to react with oxygen in steel, and cerium with both oxygen and sulfur, to form stable compounds. Aluminum oxide in small amounts is known (Ref. 11) to not affect the shape of GTA welds on 21-6-9; a similar behavior is anticipated for the cerium compounds. Thus, both Al and Ce are predicted to reduce penetration by combining with the surface active elements S and/or O and preventing them from producing a positive surface tension temperature coefficient. Ce has been shown to substantially reduce penetration in 21-6-9, and aluminum has also been shown to reduce penetration in 21-6-9 and several other stainless steels (Ref. 12).

Some observations on the affect of Al on the shape of GTA welds have appeared to be contradictory. When a steel is high in sulfur, then the surface tension temperature dependence (and hence surface tension gradients) is established by the sulfur, and removal of oxygen with aluminum has little affect on weld shape. Thus, nominal additions of over 2000 ppm aluminum to the weld pool in a Type 304N stainless steel containing 290 ppm S and exhibiting a high d/w ratio produced a negligible change in the weld pool shape (Ref. 12).

If the steel is low in sulfur, then any oxygen in the steel contributes significantly to the surface tension gradients on the weld pool. Then removal of the oxygen with aluminum alters weld pool shape, as observed on a high purity Type 304 stainless steel containing 60 ppm S (Ref. 12). Furthermore, since oxygen contents of stainless steels are often less than around 100 ppm, the effect of added aluminum would be expected to saturate after aluminum concentrations somewhat higher than 100 ppm were achieved, because most of the oxygen would be consumed. This saturation effect has also been observed (Ref. 12) in several stainless steels where there was no significant difference in the change in weld pool shape produced by nominal additions of approximately 1000 and 2500 ppm aluminum.

High speed motion pictures of GTA weld pools have demonstrated a substantial difference in fluid flow pattern between low penetration and high penetration welds—Fig. 1A. These observations led, in part, to the development of the surface tension driven fluid flow model and are consistent with it (Ref. 11). The surface fluid flow velocity has been estimated from measurements, taken from these motion pictures, of the motion of aluminum oxide particles on the weld pools. All measurements were made after sulfur was added to the weld pool so that the particles were moving toward the center of the pool. The speeds of the 17 particles measured lay between 50 and 140 cm/s (1181 and 3307 ipm), with an average speed of 94 cm/s (2220 ipm) (Ref. 12).

These speeds are consistent with those observed by Brimacombe and Weinberg (Ref. 17) for surface fluid flow on a pool of liquid tin in the presence of an imposed surface tension gradient. Additional evidence consistent with weld pool fluid flow, rather than some other effect, determining fusion zone shape is provided by the work of Mills (Ref. 18). He observed no correlation between the arc temperature distribution and fusion zone shape in 21-6-9. Furthermore, he observed (Ref. 19) that adding helium to the shielding gas broadens the arc energy distribution but produces deeper, narrower welds rather than the wider, shallower welds which might be expected from a broader heat source.

When two heats of the same stainless steel having different penetration characteristics are welded together, the point of maximum weld penetration is displaced toward the side which (when welded by itself) shows the lowest penetration (Ref. 12, 16, 20). The surface tension driven fluid flow model is consistent with this result. The lower-penetrating material has a low concentration of surface active impurities (usually sulfur) and, therefore, has a relatively high surface tension. The deeper-penetrating material has a higher concentration of surface active impurities and, therefore, a lower surface tension. Thus, there is a net surface tension gradient across the weld; consequently, surface fluid flow is across the weld pool toward the side of low-penetrating material. The result is a displacement of the weld centerline toward the low-penetrating side and maximum penetration in the low-penetrating material.

The appearance of the GTA welding arc is often visibly different in stainless steel heats exhibiting high and low penetration. This difference has led to several investigations, including those of Mills (Ref. 18, 19) discussed previously, of possible interactions between the arc and trace impurities in the base metal which could result in the observed changes in weld pool shape.

An alternate explanation for changes in arc appearance is that they result from different fluid flow patterns. If there is rapid outward surface fluid flow in the weld pool (Fig. 1A), the hottest metal in the weld pool is quickly transported away from the weld center to near the weld toe. Thus, vaporization of low vapor pressure constituents in the weld pool (especially Mn in 21-6-9) is favored over much of the weld pool surface, and a relatively wide arc results. The temperature distribution in the arc, however, appears not to be much changed, at least in 21-6-9. On the other hand, if the surface fluid flow is inward (Fig. 1B), the metal near the weld toe will be colder and metal vaporization will tend to occur nearer the center of the pool and favor a narrower arc. Thus, because of the interaction between the weld pool and the welding arc, it may be difficult to establish in a particular experiment whether the change in weld pool shape causes the change in arc characteristics or vice versa.

Finally, the work reported here demonstrates that a typical surface active addition (Se) to 21-6-9 stainless steel causes a large increase in the d/w ratio of a defocused laser weld. The observed shape change is very similar to that observed with GTA welds. This result is consistent with, and was predicted from, the surface tension driven fluid flow model. When weld penetration is by a different mechanism (as by keyhole formation in focused laser or electron beam welds), then surface tension driven fluid flow would not be expected to significantly influence penetration. The penetration of laser and electron beam welds which appear to have formed keyholes was not affected by small selenium additions to the 21-6-9 base metal.

It is not now known whether surface tension gradients are the dominant forces driving GTA weld pool fluid flow in nonferrous alloy systems. Furthermore, even in ferrous alloys, welding conditions or sample composition (so that surface tension gradients are small) may be such that

other forces are dominant. For example, as the weld current is increased, so is the magnitude of the Lorentz force; thus at high weld currents the Lorentz force may dominate surface tension forces in determining fluid flow in the weld pool.

Conclusion

The addition of small concentrations of a surface active element (Se) to 21-6-9 stainless steel dramatically increased the d/w ratio of a severely defocused, decoupled laser weld. Similar, but smaller, shape changes were observed with a defocused electron beam weld. The shape changes in the laser weld particularly were very similar to those observed previously for GTA welds when surface active elements, including Se, were added to 21-6-9.

The observation that Se produces similar shape changes in GTA welds and a defocused laser weld strongly supports the surface tension driven fluid flow model for the origin of minor element effects on GTA weld penetration. Clearly electromagnetic and possible impurity-arc interactions play no role in the defocused laser weld; however, surface tension effects are likely to be similar in the two types of weld pools.

Negligible changes in weld pool penetration or shape occurred when laser or electron beam welds crossed Se-doped zones, if weld penetration was by a keyhole mechanism. Surface tension gradients, therefore, appear to play a minor role, if any, in determining the depth and stability of the keyhole.

Acknowledgments

This work was performed under contract for the U.S. Department of Energy, Albuquerque Operations Office, whose support is gratefully acknowledged. The electron beam welding was done by V. J. Lusero and R. T. Kettl. The laser welding was performed by W. B. Estell at Sandia Livermore Laboratories. The extensive metallography was done by P. A. Kneale. Their help was greatly appreciated.

References

1. Bennett, W. S., and Mills, G. S. 1974. GTA weldability studies on high manganese stainless steel. *Welding Journal* 53 (12):548-s to 553-s.

2. Heiple, C. R., Cluley, R. J., and Dixon, R. D. 1980. Effect of aluminum on GTA weld geometries in stainless steel. *Physical metallurgy of metal joining,* eds. R. Kossowsky and M. E. Glicksman, pp. 160-165. The Metallurgical Society – AIME.

3. Makara, A. M., et al. 1977. The effect of refining on the penetration of metal in arc welding. *Automatic Weld.* 30(9):1-3.

4. Savage, W. F., Nippes, E. F., and Goodwin, G. M. 1977. Effect of minor elements on fusion zone dimensions in Inconel 600. *Welding Journal* 56(4):126-s to 132-s.

5. Oyler, G. W., Matuszesk, R. A., and Carr, C. R. 1967. Why some heats of stainless steel may not weld. *Welding Journal* 46(12):1006-1011.

6. Martin, D. C. 1955. Joining and finishing of zirconium. *The metallurgy of zirconium,* eds. B. Lustman and F. Kerze, Jr.: pp. 307-320. New York: McGraw-Hill.

7. Linnert, G. F. 1967. Weldability of austenitic stainless steel as affected by residual elements. *Effects of residual elements on properties of austenitic stainless steels,* publication no. 418:105-119. Philadelphia: Am. Soc. for Testing and Materials.

8. Patton, B. E. et al., 1974. The weldability of structural steels after refining by remelting. *Automat. Weld.* 27(6):1-4.

9. Ludwig, H. C. 1957. Arc welding of vacuum and inert-atmosphere-melted Zircaloy-2. *Welding Journal* 36(7):335-s to 341-s.

10. Heiple, C. R., and Roper, J. R. 1981. Effect of selenium on GTAW fusion zone geometry. *Welding Journal* 60(8):143-s to 145-s.

11. Heiple, C. R., and Roper, J. R. 1982. Mechanism for minor element effect on GTA fusion zone geometry. *Welding Journal* 61 (4):97-s to 102-s.

12. Heiple, C. R., and Roper, J. R. 1982. Effects of minor elements on GTAW fusion zone shape. Trends in welding research in the United States, ed. S. A. David: pp. 489-520. Metals Park, Ohio: Am. Soc. for Metals.

13. Allen, B. C. 1972. The surface tension of liquid metals. *Liquid metals – chemistry and physics,* ed. S. Z. Beer: pp. 161-212. M. Dekker, Inc.

14. Park, K., and Walter, W. F. 1979. Metal reflectance changes during intense laser irradiation. *Applications of lasers in materials processing,* E. A. Metzbower, ed., pp. 21-31. Metals Park, Ohio: American Society for Metals.

15. Heiple, C. R., Stagner, R. J., and Aden, R. J. 1980. Unpublished research.

16. Fihey, J. L., and Simoneau, R. 1982. Weld penetration variation in GTA welding of some 304L stainless steels. *Int. conf. on welding tech. for energy applications,* Gatlinburg, Tenn.

17. Brimacombe, J. K., and Weinberg, F. 1972. Observations of surface movements of liquid copper and tin. *Metall. Trans.* 3:2298-2299.

18. Mills, G. S. 1977. Analysis of high manganese stainless steel weldability problem. *Welding Journal* 56:186-s to 188-s.

19. Mills, G. S. 1979. Fundamental mechanisms of penetration in GTA welding. *Welding Journal* 58:22-s to 24-s.

20. Mosio, T., and Leinonen J. 1980. The influence of minor elements on the welding arc and penetration in austenitic stainless steel welding. *Arc physics and weld pool behavior:* pp. 285-87. Cambridge, England: The Welding Institute.